





Scheme	Step properties	
	Silicon substrate. Double-side polished, 4' diameter, 400 $\mu$ m thick, N-type 0.2 $\mu$ m thermal SiO <sub>2</sub> wet growth 0.1 $\mu$ m LPCVD Si <sub>3</sub> N <sub>4</sub> deposition	
	<b>CNM-118 HOLE mask:</b> Definition of the sensing hole 	<b>Mask</b> Hole: 5000 $\mu$ m <sup>2</sup>  <b>Step</b> 2 $\mu$ m positive photoresist 0.1 $\mu$ m Si <sub>3</sub> N <sub>4</sub> RIE etching with SF <sub>6</sub> +He 0.2 $\mu$ m SiO <sub>2</sub> wet etching (HF 49%)
	<b>CNM-118 ANCL mask:</b> Self-aligned structures 	<b>Mask</b> <b>Self aligned structure:</b> Width: 300 $\mu$ m <b>Compensation structures:</b> Width: 100 $\mu$ m Length: 700 $\mu$ m  <b>Step</b> 2 $\mu$ m positive photoresist 0.1 $\mu$ m Si <sub>3</sub> N <sub>4</sub> RIE etching with SF <sub>6</sub> +He 0.2 $\mu$ m SiO <sub>2</sub> RIE etching with CHF <sub>3</sub>
	150 $\mu$ m Si wet etching (KOH) though the window on the front layer. Back layer protected by a Teflon piece	
	Teflon piece removed. 250 $\mu$ m Si wet etching (KOH). Definition of the self-aligning structures and sensor holes	

**Table 5.11:** Technological steps for the fabrication of the piece that is self-aligned with the sensor.

So far, it has been obtained the sensor part and the aligner chip. Micromechanization has been done in both parts so as to be self-assembled during mounting. The only part of the setup that remains to be done are the V-grooves, in which both the input and output fiber optics will be located so as to easy the alignment. Technological steps that bring the definition of these structures are very similar to those for the alignment chip (Table 5.12). Process starts with a one-side polished, 400 $\mu$ m thick silicon wafer in which it is grown a 0.2 $\mu$ m silicon oxide. Afterwards, a 0.1 $\mu$ m LPCVD silicon nitride is deposited. Windows on the previously deposited layers are



opened with RIE (for the  $\text{Si}_3\text{N}_4$ ) and with HF wet etching (for  $\text{SiO}_2$ ). Silicon wafer is etched, through the windows, until a depth of  $300\mu\text{m}$ . Finally, wafer is cut using a diamond blade and fiber optics are stacked at the chips. Then, chips are polished so as to have the end of the fiber optics exactly matches the end of the V-groove.

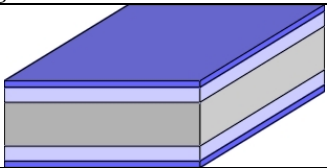
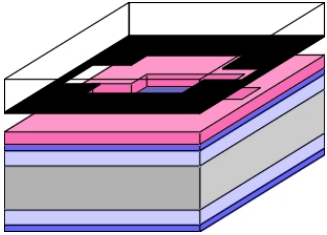
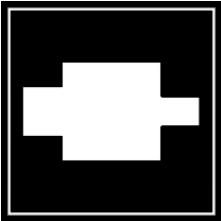
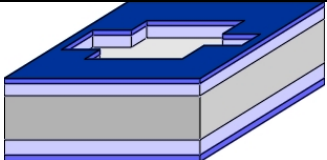
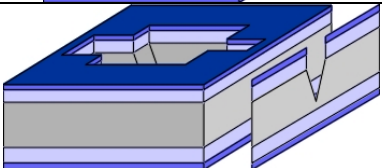
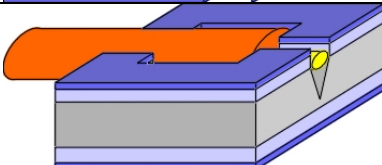
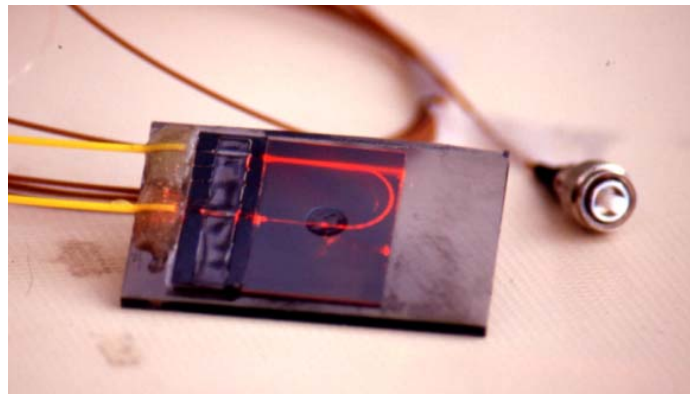
<p><b>V-grooves</b></p> 	<p>Silicon substrate. One -side polished, 4" diameter, <math>400\mu\text{m}</math> thick, N-type  <math>0.2\mu\text{m}</math> thermal <math>\text{SiO}_2</math> wet growth  <math>0.1\mu\text{m}</math> LPCVD <math>\text{Si}_3\text{N}_4</math> deposition</p>
	<p><b>CNM-119: Opening of the windows in silicon nitride</b></p> <div style="display: flex; align-items: flex-start;">  <div style="flex: 1;"> <p><b>Mask:</b>  Input width: <math>125\mu\text{m}</math>  Output width: <math>4\mu\text{m}</math></p> <p><b>Steps:</b>  <math>2\mu\text{m}</math> positive photoresist  Window definition in the <math>\text{Si}_3\text{N}_4</math> with RIE  <math>\text{SiO}_2</math> wet etching (HF 49%) through the silicon nitride window</p> </div> </div>
	<p>Wafer status after opening the windows</p>
	<p>TMAH silicon etching. <math>300\mu\text{m}</math></p>
	<p>Wafer cutting with a diamond blade  Fiber optics fixation with glue.  Polishing with SIC (<math>0.9\mu\text{m}</math>)+ <math>\text{Al}_2\text{O}_3</math> (<math>0.3\mu\text{m}</math>)</p>

Table 5.12: Technological steps for the V-groove fabrication.

Once all the required parts of the device have been obtained, the setup can be assembled. As previously mentioned, the main idea is the ability of replacing sensors fastly. Firstly, V-grooves and sensor chip are aligned, as shown in fig. 5.24, in order to analyze the correct behavior of the device. As can be seen, light injected from the input waveguides remains properly confined in the narrowest waveguide during the most



critical part of the device (bend region). When light is injected in the sensing region, the expected power loss is obtained. Outcoming power is injected to the second waveguide that, in turn, couples the light to the output fiber optics. Although this configuration is only employed for pre-alignment purposes, if both chips are glued, it could be used for sensor purposes, since it has all the necessary parts.



**Fig. 5.24:** Final appearance of the 2<sup>nd</sup> generation absorption sensor. Input and output fiber optics are placed on the same side. Light is injected by the thinner waveguide, which has a 180° bent before entering in the sensing region. Light is collected by a wider waveguide that injects light to the output fiber optic.

As can be seen in fig. 5.25, setup mounting requires several steps. Firstly, in fig. 5.25a, both single-mode and multimode fiber optics are placed on the V-groove. When the glue has dried, both fiber optics are aligned at once to the sensor (fig. 5.25b) and are mechanically blocked in this position. Then, a second V-groove is placed in top of the fiber optics, together with the micromachined piece used for self-alignment (fig. 5.25c). The two previously mentioned parts are glued to the former V-groove, allowing obtaining the basic structure (fig. 5.25d). At this point, the setup is ready to be used. If, by a given circumstance, the sensor no longer worked correctly or it was necessary to use another sensor, simply by removing it from the setup and inserting a new one should allow keep on measuring without needing an accurate alignment.

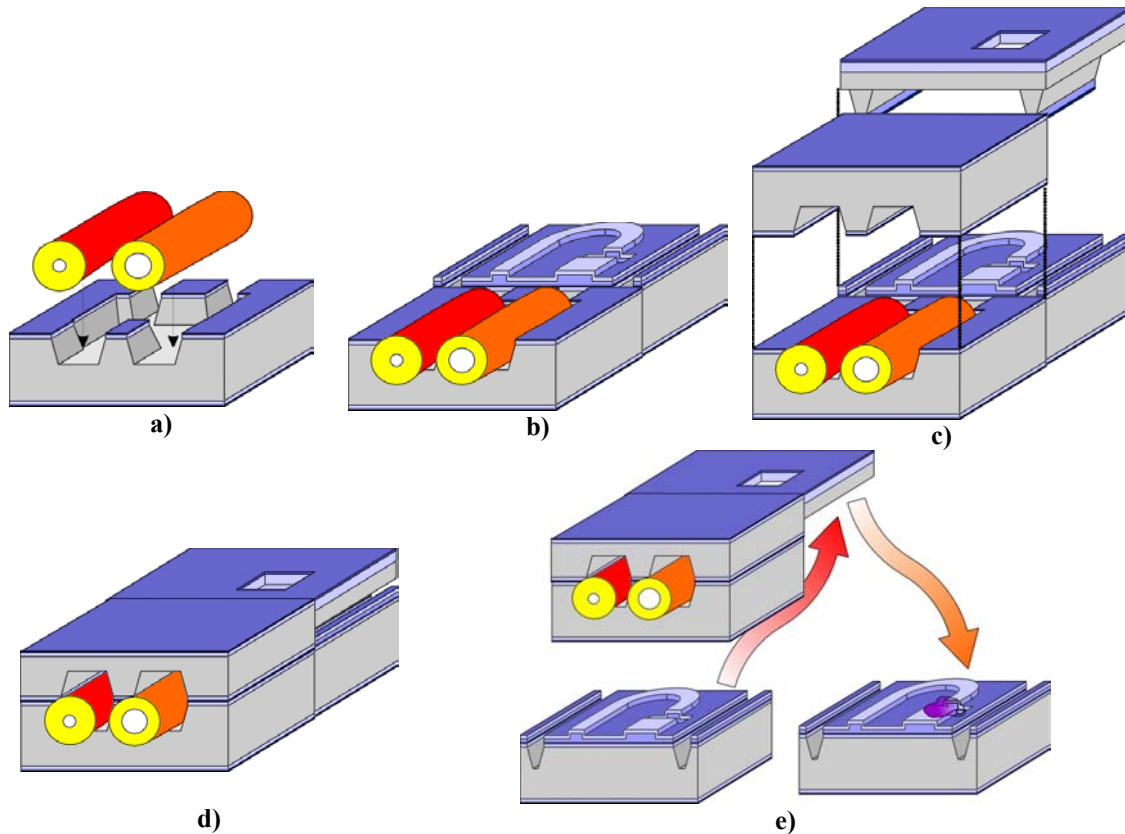


**Fig 5.25:** Absorbance sensor assembly steps. a) fiber optics mounting on V-grooves. b) fiber optics and sensor alignment. c) fixing of the upper V-groove and the self-aligner part. d) final aspect of the device (without packaging). e) changing of a malfunctioning sensor by a new one or with a membrane with different selectivity.

The final appearance of all three structures can be observed in fig 5.26a. The sensing chip does not contain a single absorption sensor, but has three of them, together with bend waveguides for testing purposes. The fact that not a unique absorption sensor was on each chip was due to two different purposes. If the same membrane was placed in all of them, it could be useful for comparison purposes. It has been observed that the sensing membrane suffers from aging by photodegradation. It was previously seen that bent waveguides with lower radius had higher losses. Thus, membranes placed with these waveguides would suffer from minor aging. Comparing the initial results of all three absorption sensors, it would be possible to know when one of them is suffering from aging. Another possibility, still in development, would be fixing a different membrane on each absorption sensor, allowing obtaining a multisensor. In fig 5.26b it is



shown a closer view of the sensing part. Through the hole done in the self-aligner chip, it can be seen the three sensing regions of the chip.

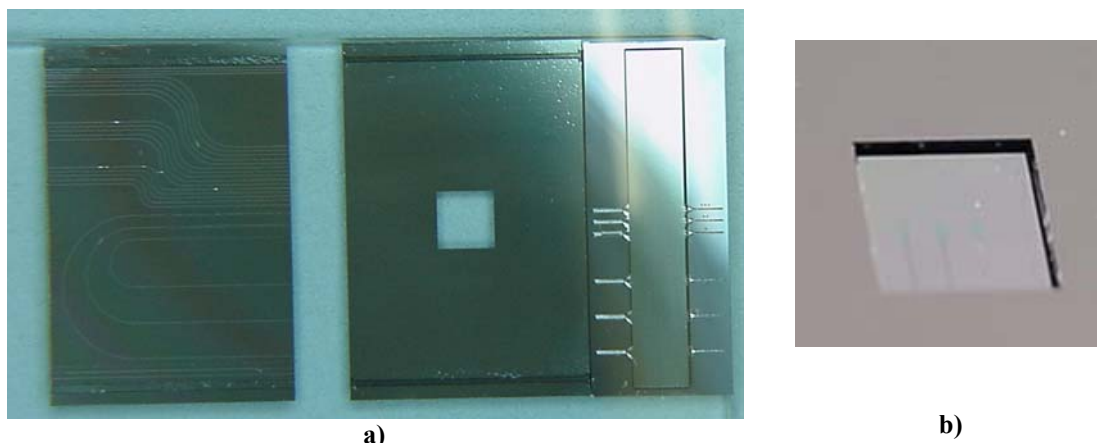


**Fig. 5.26:** a) Absorption sensor parts. b) Detail of the sensing region.

Once the fabrication steps and the assembly of the different micromechanized parts that form the absorbance sensor have been defined, its response as an optochemical sensor needs to be tested. Logically, what has been defined so far is not an optochemical sensor, but an optical transducer. As it was mentioned in chapter 4, its response as a function of the concentration of a certain ion or compound is given only by the membrane. In principle, the same device could be used for the detection of several compounds by simply varying the membrane. In practice, obtaining a membrane with a very high selectivity to a certain compound and with the selected properties is not an easy task and much effort has been put on defining new membranes.

As an example, the response of the absorption sensor as a function of the potassium-ion concentration was studied. The solution to be measured consisted in potassium chloride diluted in a 0.05M magnesium acetate buffer solution with concentrations ranging from  $10^{-4}$ M to 1M. Buffer solution was used so as to stabilize the pH of the membrane at a fixed value of 5.5. The pH value determines the quantity of available protons and, accordingly, the optimum range of  $K^{+}$  concentration for the sensor response.

Preliminary experimental results consisted in placing drops with different  $K^{+}$  concentration on the sensing region and measuring the power at each second. In figure 5.27, a comparison between a standard spectrophotometer and the absorbance sensor is



presented, as can be seen, both the absorbance range and the minimum detection values are much higher in the optochemical sensor. Maximum power at the output of this device was obtained when it was placed the buffer solution over the membrane (i.e, with no detected ions). As the droplets had more potassium-ion concentration, power dramatically decreased and after some seconds, a stable output power value was reached. Form the results obtained, it can also be seen that the dynamic range is extremely large (30dB), which represents 3 absorbance units.

As far as response time is concerned, it can be seen that changes in the output power due to variations in the  $K^+$  concentration are quite sharp at the beginning, with an asymptotic decay towards a stable value. This phenomena is according to the diffusion laws. Finally, but perhaps the most important part on this study, is that the sensor is completely reversible, that is, after the droplet that has 1M potassium-ion concentration, a cleaning with the buffer solution was done, reaching approximately the same absorbance values as previously obtained.

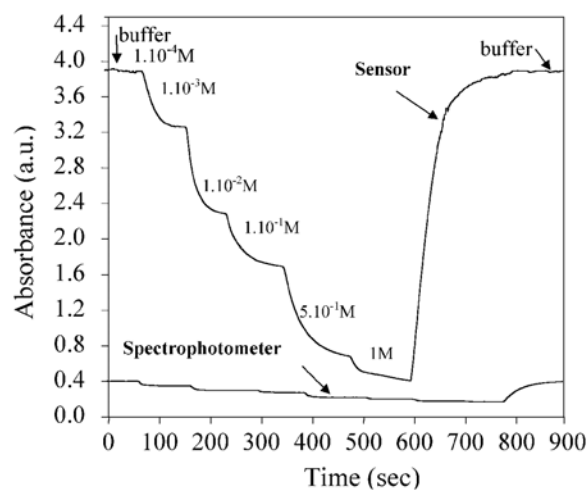


**Fig 5.27:** Comparison of the spectrophotometer and absorbance sensor as a function of the  $K^+$  concentration at a wavelength of 670nm.

Although in this work only the fabrication steps and the assembly process have been presented, a fully detailed explanation of the processes that allows obtaining the the membrane and a complete characterization of the device, not only with droplets, as has been shown here, but also with in-line configuration can be found at [7].